Talanta 138 (2015) 20–27

Contents lists available at ScienceDirect

Talanta

journal homepage: www.elsevier.com/locate/talanta

Detection and quantification of reactive oxygen species (ROS) in indoor air

V. Nahuel Montesinos [a,b,c], Mohamad Sleiman [d,e,f], Sebastian Cohn [d], Marta I. Litter [a,b,g], Hugo Destaillats [d,*]

[a] Comisión Nacional de Energía Atómica, Avenida Gral. Paz 1499, 1650 San Martín, Provincia de Buenos Aires, Argentina
[b] Consejo Nacional de Investigaciones Científicas y Técnicas, Avenida Rivadavia 1917, 1033 Ciudad Autónoma de Buenos Aires, Argentina
[c] Universidad de Buenos Aires, FCEN, INQUIMAE, DQIAQF, Ciudad Universitaria Pabellón II, 1428 Ciudad Autónoma de Buenos Aires, Argentina
[d] Lawrence Berkeley National Laboratory, Indoor Environment Group, 1 Cyclotron Road MS 70-108B, Berkeley, CA, USA
[e] Clermont Université, ENSCCF, Institut de Chimie de Clermont-Ferrand, BP 10448, F-63000 Clermont-Ferrand, France
[f] CNRS, UMR 6296, ICCF, BP 80026, F-63177 Aubière, France
[g] Universidad de General San Martín, Instituto de Investigación e Ingeniería Ambiental, Peatonal Belgrano 3563, 1650 San Martín, Pcia. Buenos Aires, Argentina

ARTICLE INFO

Article history:
Received 12 January 2015
Received in revised form
6 February 2015
Accepted 9 February 2015
Available online 14 February 2015

Keywords:
Reactive oxygen species (ROS)
Hydroxyl radical
Hydrogen peroxide
Plasma air cleaner

ABSTRACT

Reactive oxygen species (ROS), such as free radicals and peroxides, are environmental trace pollutants potentially associated with asthma and airways inflammation. These compounds are often not detected in indoor air due to sampling and analytical limitations. This study developed and validated an experimental method to sample, identify and quantify ROS in indoor air using fluorescent probes. Tests were carried out simultaneously using three different probes: 2′,7′-dichlorofluorescin (DCFH) to detect a broad range of ROS, Amplex ultra Red® (AuR) to detect peroxides, and terephthalic acid (TPA) to detect hydroxyl radicals ($HO^{\bullet}$). For each test, air samples were collected using two impingers in series kept in an ice bath, containing each 10 mL of 50 mM phosphate buffer at pH 7.2. In tests with TPA, that probe was also added to the buffer prior to sampling; in the other two tests, probes and additional reactants were added immediately after sampling. The concentration of fluorescent byproducts was determined fluorometrically. Calibration curves were developed by reacting DCFH and AuR with known amounts of H_2O_2, and using known amounts of 2-hydroxyterephthalic acid (HTPA) for TPA. Low detection limits (9–13 nM) and quantification limits (18–22 nM) were determined for all three probes, which presented a linear response in the range 10–500 nM for AuR and TPA, and 100–2000 nM for DCFH. High collection efficiency (*CE*) and recovery efficiency (*RE*) were observed for DCFH (*CE*=*RE*=100%) and AuR (*CE*=100%; *RE*=73%) by sampling from a laboratory-developed gas phase H_2O_2 generator. Interference of co-occurring ozone was evaluated and quantified for the three probes by sampling from the outlet of an ozone generator. The method was demonstrated by sampling air emitted by two portable air cleaners: a strong ozone generator (AC1) and a plasma generator (AC2). High ozone levels emitted by AC1 did not allow for simultaneous determination of ROS levels due to high background levels associated with ozone decomposition in the buffer. However, emitted ROS were quantified at the outlet of AC2 using two of the three probes. With AuR, the concentration of peroxides in air emitted by the air cleaner was 300 ppt of H_2O_2 equivalents. With TPA, the $HO^{\bullet}$ concentration was 47 ppt. This method is best suited to quantify ROS in the presence of low ozone levels.

Published by Elsevier B.V.

1. Introduction

Airborne reactive oxygen species (ROS) comprise free radicals such as hydroxyl ($HO^{\bullet}$) and peroxyl ($ROO^{\bullet}$), as well as superoxide ($O_2^{\bullet-}$) and various peroxide species. These elusive trace pollutants are often not reported in indoor air samples due to challenges associated with their collection and analysis, but are considered to be critical "stealth" environmental pollutants potentially associated with asthma and airways inflammation [1,2]. Several sampling and analytical methods using fluorescent probes have been developed recently to identify and quantify ROS in air samples. These methods have been applied to various outdoor and indoor air samples, laboratory-generated tobacco

* Corresponding author.
E-mail address: HDestaillats@lbl.gov (H. Destaillats).

http://dx.doi.org/10.1016/j.talanta.2015.02.015
0039-9140/Published by Elsevier B.V.

smoke and secondary organic aerosol particles from the ozone chemistry [3–11]. However, accurate analytical determination of ROS is still challenging, due to the instability of probes and the potential interferences with other atmospheric species. Furthermore, methods used successfully to determine high ROS concentration (such as those present in tobacco smoke and other combustion sources) may not be directly applicable to lower levels found in cleaner indoor air.

Hydroxyl radicals, peroxides and other ROS are produced in photochemically-initiated reactions, and show peak concentrations during the day in outdoor air [12]. However, the lifetime of these outdoor pollutants is too short to enable transport to indoor environments by ventilation or infiltration. Reactions with surfaces at the building envelope, indoor materials and furnishings provide an effective protection to occupants against the most reactive ROS present in outdoor air. On the other hand, various sources can contribute to the formation of ROS indoors: open combustion sources (e.g., cooking, smoking), ozone-initiated indoor chemistry and emission by "air purifying" devices whose principle of action is based on advanced oxidation processes (AOPs). Considering the latter, there is a growing interest in the use of non-thermal plasma for air cleaning applications. Microplasma systems of small size and low discharge voltage have shown good efficiency in the elimination of indoor air pollutants such as formaldehyde, albeit with simultaneous formation of ozone [13]. In general, plasma is effective in removing aerosol particles, but it has only limited efficiency in elimination of VOCs, while the formation of ozone and NO_x limits its applicability [14]. However, the combination of plasma with photocatalytic oxidation (PCO) shows an interesting synergism by integrating the fast kinetics of chemical processes initiated by the plasma with the more complete mineralization achieved by photocatalysis [15]. In addition, combined plasma and PCO systems were shown to be effective in the combined elimination of particulates (by the plasma) and gaseous pollutants (by the PCO, including the ozone produced by the plasma) [16]. The proposed mechanisms for the degradation of toluene by non-thermal plasma (DC corona discharge) showed the predominant role of $HO^{\bullet}$ in the initiation and propagation steps through addition to the aromatic ring and H-atom abstraction [17]. Plasma air cleaners were also shown to be effective in microbial inactivation [18,19]. Other air cleaning technologies may also potentially emit ROS, including those using ceramics and transition metal oxides to adsorb and/or remove formaldehyde at room temperature [20,21] and those aimed at microbial inactivation at high temperatures [22–24]. The later involves the combination of ceramic and zeolite substrates [25,26].

Fluorescent methods have been applied to the detection of ROS formed in radiation chemistry, sonochemistry, biochemistry, and on aqueous advanced oxidation processes such as PCO and photo-Fenton reactions. The fluorescence technique has been used with coumarin or terephthalic acid to detect $HO^{\bullet}$ production in PCO [27]. The method is rapid, sensitive, specific and uses simple standard instrumentation; once formed, the fluorescent product is stable and does not affect the normally occurring $HO^{\bullet}$ reactions.

In this article, three different methods are described to determine trace ROS in indoor air using fluorescent probes. One of the probes, 2′,7′-dichlorofluorescin (DCFH) was sensitive to a broad spectrum of ROS, while the other two were specific to peroxides (Amplex ultra Red®, AuR) or hydroxyl radical (terephthalic acid, TPA). The methods were validated by quantifying H_2O_2 (g) emitted in the laboratory, which allowed for comparison of their sensitivity, specificity, collection and recovery efficiencies. Interferences with ozone were also evaluated. The methods were further tested by determining the concentration of ROS emitted by two different portable air cleaners.

2. Experimental

2.1. Fluorescent probes and other reactants

The three different fluorescent probes used in this study are described in Fig. 1 and in Table 1. All chemicals used were of analytical grade or superior, and solutions were prepared using HPLC-grade water. 2′,7′-Dichlorodihydrofluorescein diacetate (H_2DCFDA) and Amplex ultra Red® (AuR) were purchased from Invitrogen™ (Carlsbad, CA). Terephthalic acid (TPA), 2-hydroxyterephthalic acid (HTPA) and other chemicals and solvents used in these tests were purchased from Sigma-Aldrich (St Louis, MO). They included Type VI – a horseradish peroxidase (HPR), a hydrogen peroxide solution (30 wt%), dimethylsulfoxide (DMSO) and phosphate buffers.

2.2. Preparation of stock solutions

For the DCFH test, a 400 μM H_2DCF solution was prepared by mixing 0.5 mL of a 10 mM H_2DCFDA ethanolic stock solution with 2 mL of NaOH 0.01 M. The hydrolysis product, H_2DCF, was kept at room temperature for 30 min and neutralized with 10 mL of 50 mM phosphate buffer (pH 7.2). This solution was freshly prepared and kept on ice prior to use. A 100 U mL^{-1} HPR solution and 1:1000 H_2O_2 stock solution were also kept on ice before use.

For the AuR test, a 10 mM AuR stock solution was prepared in DMSO and stored at −20 °C prior to use. For each experiment, this stock solution was diluted with phosphate buffer (pH 7.2, 50 mM) to prepare a fresh 150 μM AuR solution, which was stored on ice before each experiment.

For the TPA test, stock solutions for 2.5 mM HTPA and 0.5 M TPA in NaOH 0.1 M were prepared by directly dissolving the solid reactants in phosphate buffer.

All stock solutions (except 1 mM AuR) were stored in a refrigerator at 2–6 °C without showing appreciable degradation (i.e., changes in fluorescence spectra) after a month. The fluorescence

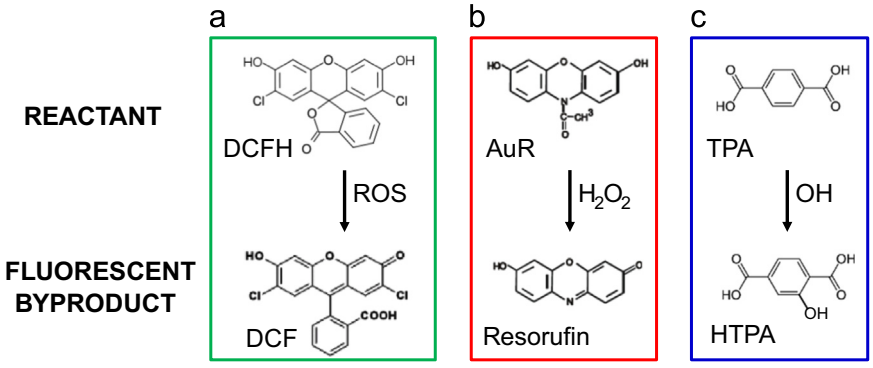

Fig. 1. Fluorescent probes used in this study. (a) 2′,7′-Dichlorofluorescin (DCFH), (b) Amplex ultra Red (AuR), and (c) terephthalic acid (TPA).

Table 1
Fluorescent probes used in ROS measurements.

Reactant	ROS detected	ROS-induced fluorescent byproduct	Excitation/ emission wavelength (nm)	Reported detection limit	Ref
2′,7′-Dichlorofluorescin (DCFH) MW: 487 CAS: 4091-99-0	H_2O_2, HO•, ROO•, $ONOO^-$	2,7-Dichloro-fluorescein (DCF) MW: 401 CAS: 76-54-0	485/530	50 nM	[8]
Amplex ultra Red® (AuR) MW: 257 CAS: 119171-73-2	H_2O_2	Resorufin MW: 213 CAS: 635-78-9	563/587	50 nM (10 pmoles)	[11]
Terephtalic acid (TPA) MW: 166 CAS: 100-21-0	HO•	2-Hydroxy-terephtalate (HTPA) MW: 181 CAS: 636-94-2	310/412	5 nM (100 fmol)	[6]

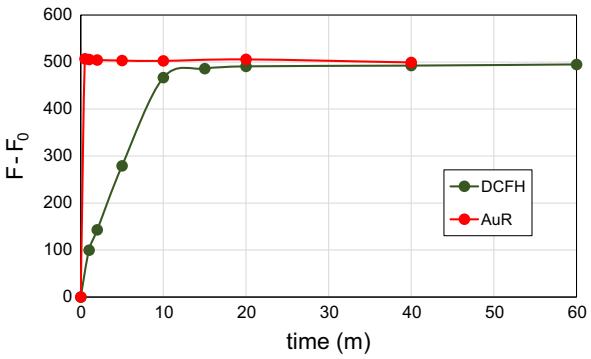

Fig. 2. Determination of the waiting period required for the reactions involving the probes DCFH and AuR. The fluorescence signal F is subtracted from the reactant blank signal, F_0.

intensity of all standards and samples collected in the tests was measured using a filter spectrofluorimeter (TD7000, Turner Design, San Jose CA) at the corresponding emission and excitation wavelengths summarized in Table 1, using 20 nm bandwidth filters. Blanks prepared using all the reactants except the fluorescent probe were carried out, and their fluorescence intensity was deducted from calibration levels on each test.

2.3. Development of calibration curves

The calibration curves for the DCFH and AuR methods were carried out with H_2O_2 solutions prepared by serial dilution of the 1:1000 H_2O_2 stock solution. For the DCFH method, a five-point calibration curve was prepared for H_2O_2 concentrations between 100 and 2000 nM. Each calibration level was prepared by addition of 400 μM H_2DCF and HPR to obtain final concentrations of 10 μM and 2 U mL^{-1}, respectively. Standards were allowed to equilibrate at room temperature in the dark for at least 20 min, to allow the reaction to be completed. The intensity of fluorescence was measured before 60 min.

The same general procedure was applied for AuR samples in the range $[H_2O_2]$ = 10–500 nM, with final concentrations of AuR and HPR of 15 μM and 1 U mL^{-1}. In this case, the reaction was almost instantaneous, and samples were equilibrated at room temperature in the dark for only 3–5 min. The fluorescent intensity was measured before 30 min, and the signal was confirmed to be stable for at least 40 min. Fig. 2 shows measurements taken at different times to determine the duration of the equilibration period required for the reaction to be completed and the stability of the fluorescent signals for these two probes.

In the case of TPA tests, calibration curves were developed using directly the fluorescent species, HTPA, the ROS-induced compound. Dilutions were prepared from a stock HTPA solution of 2.5 mM, in the range 10–500 nM. Fig. 3 presents the calibration curves prepared for each of the three fluorescent probes.

The analytical and statistical parameters for these calibrations are presented in Table 2. All calibration curves were successfully

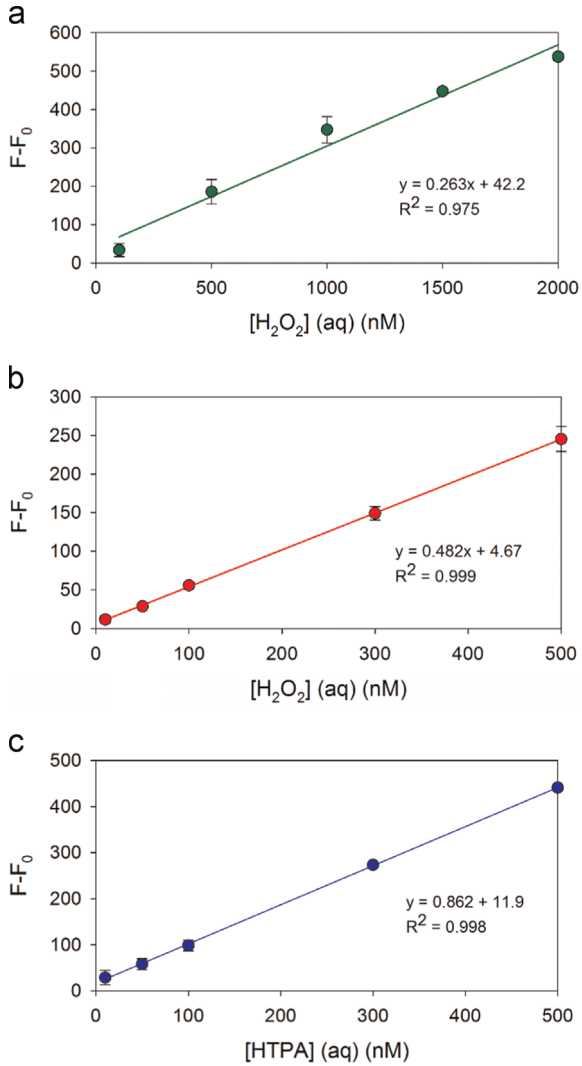

Fig. 3. Calibration curves determined with the three fluorescent probes in aqueous solution: (a) DCFH, (b) AuR, and (c) TPA.

Table 2
Analytical figures of merit for ROS quantification using DCFH, AuR and TPA.

Probe	Slope (nM^{-1})	RSD (%)	DL (nM)	QL (nM)	Lowest calibration level
DCFH	0.27	2.9	9.1	15.2	100 nM H_2O_2
AuR	0.48	6.4	13.2	22.0	10 nM H_2O_2
TPA	0.86	3.0	10.9	18.3	10 nM HTPA

adjusted by a linear correlation with $R^2 \geq 0.98$. The detection limit (DL) and quantification limit (QL) were calculated for each probe, based on instrumental response. The instrumental limits were calculated as three (DL) or five (QL) times the standard deviation of the

blank. In all cases, DL and QL obtained were in good agreement with those showed in prior studies using the same probes (see references in Table 1). The good reproducibility for each method is reflected by the low Slope Relative Standard Deviation (RSD), which were in all cases lower than 7%. Finally, it was observed that the reaction time of AuR was significantly faster than that of DCFH, and that the fluorescent product was more stable.

2.4. Development of the ROS sampling method

2.4.1. Validation using a stable H_2O_2 (g) source

Various methods reported in the literature use only aqueous H_2O_2 solutions to develop a calibration. However, capturing H_2O_2 (and other ROS) from air into an aqueous system may be affected by losses that need to be quantified. Tests were performed in the laboratory using a stable gas-phase ROS source to characterize the accuracy of the determination and the collection efficiency. Each ROS sample was collected by bubbling H_2O_2-enriched air into two impingers in series containing the corresponding buffer used for analysis of each fluorescent probe. The ROS source consisted of a bubbler containing a known concentration of H_2O_2, $[H_2O_2]$ (aq) in equilibrium with the corresponding gas phase concentration $[H_2O_2]$ (g). The peroxide generator and ancillary sampling equipment are illustrated in Fig. 4. A controlled flow of clean air ("zero" quality, Praxair, CA) was bubbled first through a water column to achieve saturation, and then through a gas sparger consisting of a glass column provided with a porous frit base that was filled with 250 mL of a H_2O_2 aqueous solution of known concentration, in the range $[H_2O_2]$ (aq)=1–13 mM. For the evaluation of the DCFH and AuR methods, gas phase H_2O_2 was collected in two 25 mL Midget Impingers (SKC®, California) in series filled with 10 mL of 50 mM phosphate buffer (pH 7.2) kept in an ice bath at a constant temperature of 3 °C to maximize peroxide capture and prevent ROS decomposition in aqueous solution. After collection, a 3 mL aliquot from each impinger was placed in a 5 mL volumetric flask, the reactants (including the fluorescent probe) were added immediately after sampling, and the fluorimetric assays were carried out following the same procedure described above for the calibration standards. For the TPA test, 10 mL of 0.5 mM TPA in 50 mM phosphate buffer (pH 7.2) solution was placed in each impinger. In this case, the fluorimetric determination was carried out without further dilution of the collected sample. In all cases the corresponding blanks were prepared by bubbling "zero quality" clean air into the impingers containing the corresponding probes. A calibration curve for each probe was also prepared and analyzed simultaneously.

2.4.2. Effect of ozone on ROS sampling

Often, ROS sampling takes place in the presence of atmospheric ozone. For that reason, this study evaluated potential sampling artifacts that can be attributed to the presence of ozone. Experiments were carried out for each of the three probes. In each case, two impingers in series containing the corresponding sampling buffers were connected downstream of an ozone generator (OG-2, UVP, Upland CA), which was fed with "zero" quality clean air to produce controlled gas phase concentrations of O_3 in the range 13–470 ppbv. The low-end of this range corresponded to typical indoor ozone values, and the high-end to levels that may be reached in a small indoor space using a commercial ozone-generating air cleaning device. In all cases, 50–60 L samples were collected by drawing air at rates of 0.85–0.75 L min^{-1}. Ozone concentrations were determined using a photometric ozone analyzer (Advanced Pollution Instrumentation Inc., San Diego CA), and ROS were quantified fluorometrically in duplicate determinations following the above-described protocol.

2.5. Determination of ROS concentrations emitted by a portable air cleaner

Two different portable air cleaning devices were used to evaluate the emission of ROS. The first one (air cleaner AC1) consisted of a fan forcing room air through a PCO catalyst irradiated by an ozone-generating UV lamp, at an air flow of 10 m^3 h^{-1}. It was advertised as a residential air purifier and sanitizer, targeting mold, bacteria, viruses, odors and VOCs. The other device (air cleaner AC2), comprised a fan that circulated room air through a plasma generator, at a flow rate of 8 m^3 h^{-1}. It was advertised as an air purifier targeting airborne microorganisms. ROS and ozone were sampled simultaneously under identical conditions at the outlet of both air cleaners. Two impingers in series were placed directly at the outlet of each device, and outcoming air was sampled at flow rates between 0.5 and 1 L min^{-1}. Custom-made aluminum foil ducting was used to ensure that air exiting each device was not mixed with room air prior to sampling. A 3 mL aliquot of the collected sample was used at the end of each test to determine the amount of ROS emitted by each air cleaner and by the ozone generator as described above.

3. Results and discussion

3.1. Collection and recovery efficiencies

In the experiment using the stable H_2O_2 source, and assuming that the gas/liquid partitioning was achieved instantaneously, the

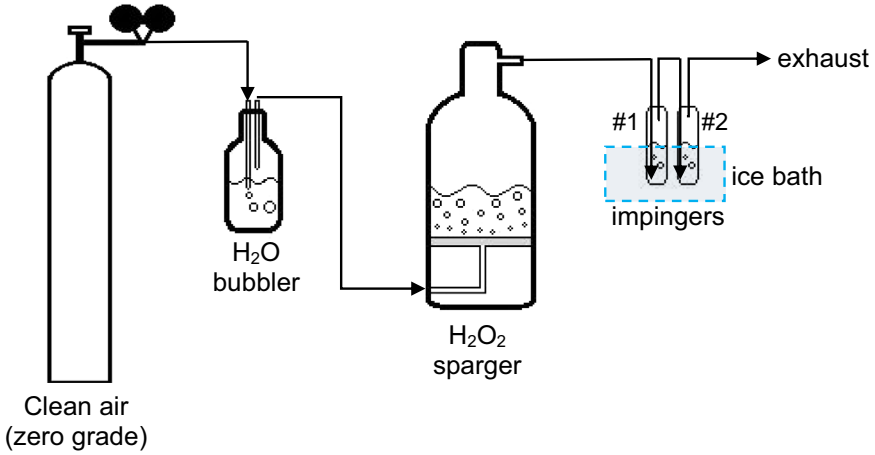

Fig. 4. Experimental setup used to develop the ROS sampling method.

Table 3
Experimental conditions and results for H_2O_2 collection efficiency with each fluorescent probe.

Probe	T (°C)	$[H_2O_2]$ (aq) (mM)	Sampling time (min)	Sampling flow rate (L min^{-1})	Expected[a] $[H_2O_2]$ (g) (ppb)	Measured $[H_2O_2]$ (g) (ppb)	CE (%)	RE (%)
DCFH	12–14	12.7	23	0.70	35–49	42 ± 1	100	100
AuR	12–14	1.27	30	0.75	3.8–4.7	3.1 ± 1.1	100	73
TPA	12–14	12.7	30	0.70	35–49	n.d.	N/A	0

[a] Calculated as the product of the aqueous concentration.

aqueous peroxide concentration, $[H_2O_2]$ (aq), was used to estimate the expected concentrations in the gas phase, $[H_2O_2]$ (g). For this calculation, the value of Henry's law constant of H_2O_2 in water at infinite dilution at 288 K and pH 7 used was $K_H^{\infty} = 2.4 \times 10^5$ M atm^{-1} [28]. The experimental conditions are indicated in Table 3. The collection flow rates and peroxide concentrations inside the sparger were adjusted to fit in the linear range of each technique when using a sampling time of approximately 30 min. Tests were carried out for the AuR, DCFH and TPA methods to evaluate the overall recovery efficiency of gas phase H_2O_2 by the sampling system and to calculate the collection efficiency at the first impinger (CE) determined as follows:

$$CE = 100\left[1 - \frac{[H_2O_2]\,(g,\ \text{impinger 2})}{[H_2O_2]\,(g,\ \text{impinger 1})}\right] \quad (1)$$

where $[H_2O_2]$ (g, impinger 1) and $[H_2O_2]$ (g, impinger 2) are the H_2O_2 gas phase concentrations determined with data from the first and the second impinger, respectively (as described below in more detail). Results reported in Table 3 show that, for DCFH and AuR, the collection efficiency was $CE = 100\%$, indicating that there was no breakthrough of analyte to the second impinger under the working conditions. Furthermore, the tests also showed excellent recovery efficiencies (RE) for both probes, as determined by the following:

$$RE = 100\left[\frac{\text{measured } [H_2O_2]\,(g)}{\text{expected } [H_2O_2]\,(g)}\right] \quad (2)$$

The H_2O_2 gas phase concentrations were within the expected values calculated with the Henry´s law constant in the case of DCFH (i.e., $RE = 100\%$). For AuR, the measured value was slightly lower than the expected range of concentration, consistent with a recovery of $RE = 73\%$. One possible reason for the incomplete recovery may be the fact that this test was carried out with H_2O_2 concentrations 10 times lower than those used for DCFH tests, and the determination involved larger uncertainties (the relative error for DCHF was ~3%, and for AuR it was 35%). Blank experiments without H_2O_2 in the sparger showed no fluorescent signal for both probes. The test performed with TPA did not generate any measureable amount of HTPA, as expected, since this probe is not sensitive to H_2O_2. The negative result obtained with TPA confirmed that this probe is not sensitive to peroxides.

3.2. Ozone interferences

Ozone has a complex chemistry in aqueous solution that, under most conditions, leads to the formation of hydroxyl radicals, peroxides and superoxide [29]. These species can react with one or more fluorometric probes and cause sampling interferences. A simplified scheme illustrating the main chemical processes is shown in Fig. 5.

The results of laboratory tests to evaluate the effect of ozone in ROS sampling are illustrated in Fig. 6. The total amount of O_3 (from an ozone generator) bubbled through the impingers is plotted against the equivalent aqueous hydrogen peroxide concentration, $[H_2O_2]^{eq}$ (aq), measured in the sampling solutions at the end of the

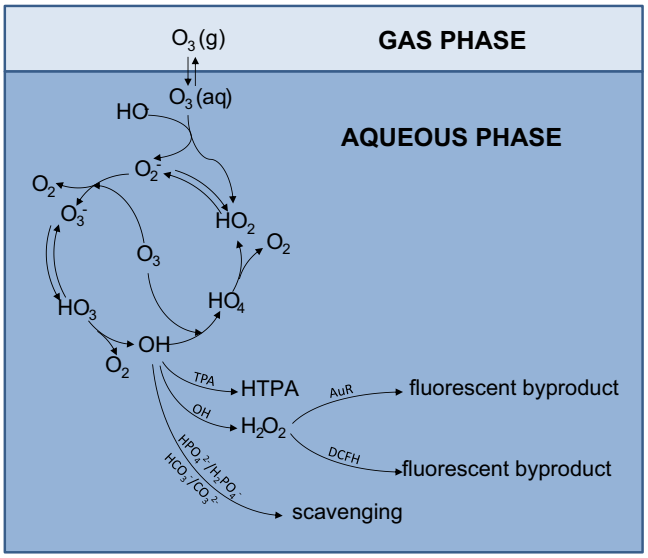

Fig. 5. Schematic representation of chemical processes in aqueous solution leading to the formation of ROS from ozone decomposition.

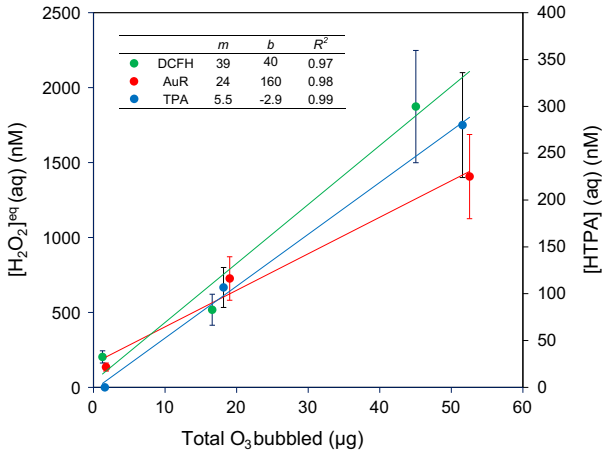

Fig. 6. Equivalent H_2O_2 and HTPA concentrations determined in the presence of ozone.

DCFH and AuR tests (represented in the left y-axis). The superscript "eq" (equivalent) denotes that we report as H_2O_2 not only this compound but also any other ROS that reacts with the probe leading to the formation of the fluorescent byproduct. The aqueous peroxide equivalent concentration $[H_2O_2]^{eq}$ (aq) was determined as the sum of values determined in impingers 1 and 2 (expressed in nM), to account for breakthrough (if $RE < 100\%$), as follows:

$$[H_2O_2]^{eq}\,(aq) = [H_2O_2]^{eq}\,(aq,\ \text{impinger 1}) + [H_2O_2]^{eq}\,(aq,\ \text{impinger 2}) \quad (3)$$

Results from the TPA tests are plotted in terms of aqueous HTPA concentrations (in the right *y*-axis). Similarly, [HTPA] (aq) was determined as the sum of values measured in both impingers:

$$[\text{HTPA}]\,(\text{aq}) = [\text{HTPA}]\,(\text{aq, impinger 1}) + [\text{HTPA}]\,(\text{aq, impinger 2}) \quad (4)$$

In all cases, linear trends with slope m and intercept b were derived, as reported in Fig. 6. These linear correlations suggest that the measured signal is proportional to the amount of ozone circulated through the aqueous medium. DCFH showed the highest response for the same amount of O_3 bubbled, in good agreement with the fact that it can react with a broad variety of ROS produced upon decomposition of dissolved O_3. Instead, AuR and TPA reacted with peroxides and $HO^{\bullet}$, respectively. It can be assumed that AuR reacted primarily with the main stable peroxide generated by O_3 in water, H_2O_2. In the case of TPA, it detected the $HO^{\bullet}$ radicals generated during that process. The linear correlations from Fig. 6 were used to subtract the contribution of dissolved O_3 on the measured ROS concentrations. The amount of O_3 bubbled was calculated directly from the O_3 (g) concentration measured at the outlet of the air cleaner during ROS sampling.

Further evidence of the role played by dissolved ozone in ROS sampling artifacts was obtained from carrying out these determinations at different sampling temperatures, in the range 3–18 °C. Ozone solubility decreased with increasing temperature of the sampling buffer, leading to a reduction in the amount of ROS detected. The total amount of ROS captured, expressed in equivalent H_2O_2 aqueous concentration in the impingers, $[H_2O_2]^{eq}$ (aq), was measured in each case with the DCFH method and correlated with the expected decrease in ozone solubility, as shown in Fig. 7. In each of these three tests, the concentration of ozone in the air circulating through the impingers was 470 ppb, and the volume of air sampled in each case over approximately one hour was 50 L. A marked effect of the buffer temperature was observed, suggesting that ozone dissolution was the main factor driving the formation of ROS in the system. When temperature increased, the total amount of dissolved ozone decreased and, with it, the amount of ROS generated in the impingers.

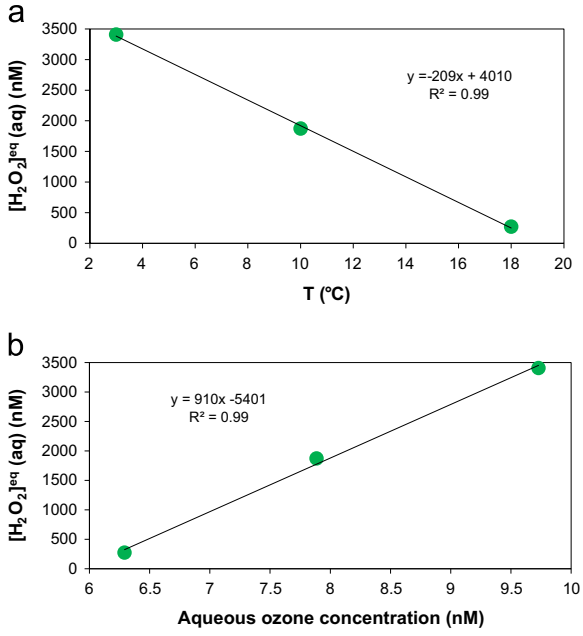

Fig. 7. Equivalent aqueous H_2O_2 concentration determined with the DCFH method at three collection temperatures, by sampling 50 L of air containing 470 ppb O_3 (g). (a) Effect of temperature and (b) Effect of O_3 (aq) concentration.

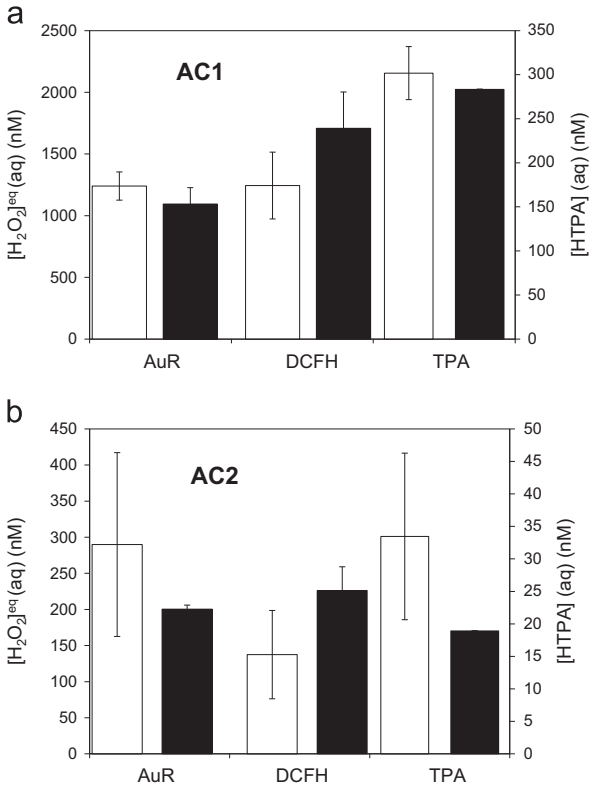

Fig. 8. Equivalent aqueous H_2O_2 and HTPA concentrations determined for the air cleaners (white) and for an ozone generator (black). (a) AC1; (b) AC2.

3.3. Determination of ROS emitted by two portable air cleaners

The results corresponding to tests carried out with the two air cleaners are presented in Fig. 8. The white bars reflect the amount of $[H_2O_2]^{eq}$ (aq) or [HTPA] (aq) measured by bubbling air from the outlet of each device, whereas the black bars are the expected signal calculated from the linear expressions shown in Fig. 6 using the amount of O_3 bubbled in each experiment. In the case of the air cleaner AC1, although the overall response was higher, all the ROS signal could be attributed to the formation of ROS in solution due to the presence of ozone. The concentration of ozone measured at the outlet of the air cleaner was 455 ± 20 ppb. Given the high level of ozone emitted by this device and the concomitant high background ROS signal, it was not possible to quantify ROS that may be emitted simultaneously with ozone. The calculated signal for the DCFH method yielded a higher expected value for ozone than that obtained for the air cleaner. While the other two methods showed a slightly higher signal for the air cleaner than for the ozone generator, the relative differences were only 6% for TPA and 11% for AuR, which were of the same order of the experimental error.

In the case of the air cleaner AC2 (plasma generator), the concentration of ozone measured at the outlet was much lower, 36 ± 14 ppb. Similar to results observed for AC1, the ROS expected signal for DCFH was higher than that for the air cleaner. However, measurements for the other two probes (TPA and AuR) showed ROS levels for emissions from the air cleaner that were significantly higher than background levels at the same ozone concentration (43% and 31% higher, respectively, see Fig. 8). In consequence, the contribution of airborne ROS from AC2 could be estimated by subtracting the value determined with the air cleaner from the contributions predicted from ozone decomposition.

Table 4
Determination of ROS levels emitted by plasma air cleaner AC2.

Peroxides by AuR method		Hydroxyl radical by TPA method	
$[H_2O_2]^{eq}$ (aq, air cleaner) (nM)	290 ± 130	[HTPA] (aq, air cleaner) (nM)	33 ± 12
$[H_2O_2]^{eq}$ (aq, ozone) (nM)	200 ± 10	[HTPA] (aq, ozone) (nM)	19 ± 1
$[H_2O_2]^{eq}$ (aq, plasma) (nM)	90 ± 140	[HTPA] (aq, plasma) (nM)	14 ± 13
$[H_2O_2]^{eq}$ (g) (ppt)	**300 ± 300**	**[HO•] (g) (ppt)**	**47 ± 46**

The quantification of ROS emissions by AC2 is summarized in Table 4. Values were determined as follows:

3.3.1. AuR

The aqueous peroxide equivalent concentration corresponding to ROS emitted by the plasma process, $[H_2O_2]^{eq}$ (aq, plasma), was determined by subtracting the expected ROS produced from O_3 decomposition from the value determined from the air cleaner:

$$[H_2O_2]^{eq}\,(\text{aq, plasma}) = [H_2O_2]^{eq}\,(\text{aq, air cleaner}) - [H_2O_2]^{eq}\,(\text{aq, ozone}) \quad (5)$$

The number of moles of peroxide emitted to the gas phase, n_{H2O2} was calculated by multiplying this value by the volume of buffer used to collect the sample (V=10 mL), as follows:

$$n_{H2O2} = V\,[H_2O_2]^{eq}\,(\text{aq, plasma}) \quad (6)$$

The gas phase concentration (in part-per-trillion units, ppt) was calculated as follows:

$$[H_2O_2]^{eq}\,(g) = n_{H2O2}\left(\frac{V_m}{V_{air}}\right)10^{12} \quad (7)$$

where V_m is the the molar volume of air at standard conditions of temperature and pressure (22.4 L mol^{-1}), and V_{air} is the volume of air sampled (in L).

3.3.2. TPA

The aqueous HTPA concentration corresponding to ROS emitted by the plasma process, [HTPA] (aq, plasma) was determined by subtracting the expected ROS produced from O_3 decomposition from the value determined from the air cleaner:

$$[\text{HTPA}]\,(\text{aq, plasma}) = [\text{HTPA}]\,(\text{aq, air cleaner}) - [\text{HTPA}]\,(\text{aq, ozone}) \quad (8)$$

The number of moles of hydroxyl radicals emitted to the gas phase, n_{HO}, was calculated by multiplying this value by the volume of buffer used to collect the sample, as follows:

$$n_{HO} = V\,[\text{HTPA}]\,(\text{aq, plasma}) \quad (9)$$

and the concentration of HO• radicals in the gas phase (in part-per-trillion units, ppt) was calculated as follows:

$$[HO^{\bullet}]\,(g) = n_{HO}\left(\frac{V_m}{V_{air}}\right)10^{12} \quad (10)$$

The levels reported in Table 4, measured directly at the outlet of the devices, can be considered an upper limit for indoor concentrations, since additional losses may occur due to fast deposition to indoor surfaces and gas phase reactions. These levels can be put into perspective by comparing with levels of H_2O_2 and HO• radicals reported in indoor and outdoor air. Hydrogen peroxide concentrations between 500 ppt and 3.5 ppb have been reported in urban air, mainly in the gas phase [4]. Similar levels of up to 5 ppb have been reported in non-urban tropospheric measurements [30]. Considering indoor environments, gas phase peroxides, generated from reaction of ozone with D-limonene in an office with a strong ozone source, have been measured in the range 0.6–1.5 ppb [31]. These reported indoor and outdoor levels are of the same magnitude as those measured in this study for the air cleaner AC2. Unfortunately, the high background levels prevented us to measure ROS emissions from AC1. In that case, it is likely that peroxide emissions occurring simultaneously with ozone emissions were of similar magnitude or higher than those from ozone–terpene chemistry.

In the case of hydroxyl radicals, typical daytime outdoor levels are $\sim 10^6$ cm^{-3} ($\sim 10^{-1}$ ppt), and peak above $\sim 10^7$ cm^{-3} (~ 1 ppt) in polluted urban atmospheres [32]. While outdoor/indoor transport is negligible due to their very low lifetimes, indoor levels are often in the range of 10^5 cm^{-3}, mostly due to indoor sources [33,34]. However, recent studies reported higher levels that approach those measured outdoors [35]. In chamber studies with high ozone and terpene concentrations, HO• radical concentrations of up to $\sim 10^7$ cm^{-3} (~ 1 ppt) were measured [36]. In this study, assuming that radical species reacting with TPA were exclusively HO• radicals, values measured directly at the outlet of the plasma generator (AC2) were between one and two orders of magnitude higher than HO• levels recorded in outdoor air. It is expected that these concentrations will be reduced rapidly in indoor environments due to recombination processes in the gas phase, reactions with VOCs and with indoor surfaces. However, breathing air in the proximity of the device – where samples for this study were taken – will likely lead to exposure to elevated levels of HO• radicals.

4. Conclusions

This study developed and validated an experimental approach to compare several analytical methods that measure ROS in indoor air using fluorescent probes. Different reactivity and specificity for each probe towards different ROS species were demonstrated. It also developed a simple and reliable validation process using H_2O_2 gas phase and demonstrated that ROS can be detected in the air emitted by portable air purifiers. The methods described here are useful to quantify high levels of indoor ROS, such as those emitted by certain air cleaning devices, particularly in the absence of high ozone levels. It should be kept in mind that ozone interferences may lead to misclassifications and “false positive” ROS determinations. For that reason, these probes should also be used in combination with conventional ozone measurements and can be powerful analytical tools to elucidate mechanisms of AOTs either in the gas or in the aqueous phase.

Acknowledgments

This study was funded by the California Air Resources Board (CARB) through Agreement no. 10-320. It was carried out at Lawrence Berkeley National Laboratory (LBNL), which operates under U.S. Department of Energy Contract DE-AC02-05CH11231. The authors thank P. Jenkins, M. Gabor and Q. Zhang of CARB’s Research Division for their inputs, review and effective technical management. We also acknowledge valuable suggestions from W. Fisk (LBNL), S. Paulson (UCLA) and T. Kirchstetter (LBNL), and the experimental contributions of M. Russell (LBNL). The statements and conclusions in this study are those of the contractor and not necessarily those of CARB. The mention of commercial products, their source, or their use in connection with material reported herein is not to be construed as actual or implied endorsement of such products. VNM and MIL were supported by Agencia Nacional de Promoción Científica y Tecnológica (Argentina), project PICT-0463.

References

[1] C.J. Weschler, Environ. Health Perspect. 114 (2006) 1489–1496.
[2] C.J. Weschler, J.R. Wells, D. Poppendieck, H. Hubbard, T.A. Pearce, Environ. Health Perspect. 114 (3) (2006) 442–446.
[3] C. Arellanes, S.E. Paulson, P.M. Fine, C. Sioutas, Environ. Sci. Technol. 40 (2006) 4859–4866.
[4] A.S. Hasson, S.E. Paulson, J. Aerosol Sci. 34 (2003) 459–468.
[5] S.B. Hong, G.S. Kim, C.H. Kang, J.H. Lee, Environ. Monit. Assess. 147 (2008) 23–34.
[6] L. Linxiang, Y. Abe, Y. Nagasawa, R. Kudo, N. Usui, K. Imai, T. Mashino, M. Mochizuki, N. Miyata, Biomed. Chromatogr. 18 (2004) 470–474.
[7] M. Sleiman, H. Destaillats, L.A. Gundel, Talanta 116 (2013) 1033–1039.
[8] P. Venkatachari, P.K. Hopke, Aerosol Sci. Technol. 42 (2008) 629–635.
[9] Y. Wang, H. Kim, S.E. Paulson, Atmos. Environ. 45 (2011) 3149–3156.
[10] J. Zhao, P.K. Hopke, Aerosol Sci. Technol. 46 (2012) 191–197.
[11] M. Zhou, Z. Diwu, N. Panchuk-Voloshina, R.P. Haugland, Anal. Biochem. 253 (1997) 162–168.
[12] B.J. Finlayson-Pitts, J.N. Pitts, Chemistry of the Upper and Lower Atmosphere, Academic Press, San Diego, CA (2000) 969.
[13] K. Shimizu, M. Blajan, T. Kuwabara, IEEE Trans. Ind. Appl. 47 (2011) 2351–2357.
[14] Y. Zhang, J. Mo, Y. Li, J. Sundell, P. Wargocki, J. Zhang, J.C. Little, R. Corsi, Q. Deng, M.H.K. Leung, L. Fang, W. Chen, J. Li, Y. Sun, Atmos. Environ. 45 (2011) 4329–4343.
[15] F. Thevenet, O. Guaitella, E. Puzenat, J.-M. Herrmann, A. Rousseau, C. Guillard, Catal. Today 122 (2007) 186–194.
[16] J.H. Park, J.H. Byeon, K.Y. Yoon, J. Hwang, Indoor Air 18 (2008) 44–50.
[17] J. Van Durme, J. Dewulf, W. Sysmans, C. Leys, H. Van Langenhove, Chemosphere 68 (2007) 1821–1829.
[18] Y.D. Liang, Y. Wu, K. Sun, Q. Chen, F.X. Shen, J. Zhang, M.S. Yao, T. Zhu, J. Fang, Environ. Sci. Technol. 46 (2012) 3360–3368.
[19] H. Nishikawa, H. Nojima, Sharp Tech. J. 86 (2003) 10–15.
[20] M.A. Sidheswaran, H. Destaillats, D.P. Sullivan, J. Larsen, W.J. Fisk, Appl. Catal. B—Environ. 107 (2011) 34–41.
[21] J.G. Yu, X.Y. Li, Z.H. Xu, W. Xiao, Environ. Sci. Technol. 47 (2013) 9928–9933.
[22] B. Damit, C.Y. Wu, M.S. Yao, J. Aerosol Sci. 65 (2013) 88–100.
[23] J.H. Jung, J.E. Lee, S.S. Kim, Sci. Total Environ. 407 (2009) 4723–4730.
[24] J.H. Jung, J.E. Lee, S.S. Kim, G.N. Bae, J. Aerosol Sci. 41 (2010) 602–610.
[25] H.H. Cheng, C.C. Hsieh, C.H. Tsai, Aerosol Air Qual. Res. 12 (2012) 409–419.
[26] J.H. Ji, G.N. Bae, S.H. Yun, J.H. Jung, H.S. Noh, S.S. Kim, Aerosol Sci. Technol. 41 (2007) 786–793.
[27] K.-I. Ishibashi, A. Fujishima, T. Watanabe, K. Hashimoto, Electrochem. Commun. 2 (2000) 207–210.
[28] D. Huang, Z. Chen, J. Environ. Sci. 22 (4) (2010) 570–574.
[29] H. Destaillats, A.J. Colussi, J.M. Joseph, M.R. Hoffmann, J. Phys. Chem. A 104 (2000) 8930–8935.
[30] R. Balasubramanian, L. Husain, J. Geophys. Res. 102 (D17) (1997) 21,209–21,220.
[31 T.H. Li, B.J. Turpin, H.C. Shields, C.J. Weschler, Environ. Sci. Technol. 36 (2002) 3295–3302.
[32] S. Dusanter, D. Vimal, P.S. Stevens, R. Volkamer, L.T. Molina, Atmos. Chem. Phys. 9 (2009) 1665–1685.
[33] B.C. Singer, B.K. Coleman, H. Destaillats, A.T. Hodgson, M.M. Lunden, C.J. Weschler, W.W. Nazaroff, Atmos. Environ. 40 (2006) 6696–6710.
[34] C.J. Weschler, H.C. Shields, Environ. Sci. Technol. 31 (1997) 3719–3722.
[35] S. Gligorovski, C.J. Weschler, Environ. Sci. Technol. 47 (2013) 13905–13906.
[36] H. Destaillats, M.M. Lunden, B.C. Singer, B.K. Coleman, A.T. Hodgson, C.J. Weschler, W.W. Nazaroff, Environ. Sci. Technol. 40 (2006) 4421–4428.